MORTIER, W. J., SAUER, J., LERCHER, J. A. & NOLLER, H. (1984). *J. Phys. Chem.* **88**, 905–912.
OHASHI, Y. & FINGER, L. W. (1981). *Am. Mineral.* **66**, 154–168.
PARISE, J. B., CORBIN, D. R., ABRAMS, L. & COX, D. E. (1984). *Acta Cryst.* C**40**, 1493–1497.
PARISE, J. B. & DAY, C. S. (1985). *Acta Cryst.* C**41**, 515–520.
PARISE, J. B., GIER, T. E., CORBIN, D. R. & COX, D. E. (1984). *J. Phys. Chem.* **88**, 1635–1640.
PERSSON, J., FRECH, W. & CEDERGREN, A. (1977). *Anal. Chim. Acta*, **92**, 85–93.
PLUTH, J. J. & SMITH, J. V. (1982). *J. Am. Chem. Soc.* **104**, 6977–6982.
RIETVELD, H. M. (1969). *J. Appl. Cryst.* **2**, 65–71.
ROBSON, H. E., SHOEMAKER, D. P., OGILVIE, R. A. & MANOR, P. C. (1973). In *Molecular Sieves*, Advances in Chemistry Series No. 121, edited by W. M. MEIER & J. B. UYTTERHOEVEN, pp. 106–115. Washington, DC: American Chemical Society.
ROGOWSKI, D. F., ENGLISH, A. J. & FONTIJN, A. J. (1986). *J. Phys. Chem.* **90**, 1688–1691.
ROSSI, G., TAZZOLI, V. & UNGARETTI, L. (1974). *Am. Mineral.* **59**, 335–340.
ROTELLA, F J. (1982). *Users Manual for Rietveld Analysis of Time-of-Flight Neutron Powder Data at IPNS*. Argonne: Argonne National Laboratory.
SCHMID, R. L., FELSCHE, J. & MCINTYRE, G. J. (1984). *Acta Cryst.* C**40**, 733–736.
SCHMID, R. L., FELSCHE, J. & MCINTYRE, G. J. (1985). *Acta Cryst.* C**41**, 638–641.
SCHMID, R., HUTTNER, G. & FELSCHE, J. (1979). *Acta Cryst.* B**35**, 3024–3027.
SCHMID, R. L., SZOLNAI, L., FELSCHE, J. & HUTTNER, G. (1981). *Acta Cryst.* B**37**, 789–792.
SHANNON, R. D. (1976). *Acta Cryst.* A**32**, 751–767.
SHANNON, R. D., GARDNER, K. H., STALEY, R. H., BERGERET, G., GALLEZOT, P. & AUROUX, A. (1985). *J. Phys. Chem.* **89**, 4778–4788.
SMOLIN, YU. I., SHEPELEV, YU. F. & BUTIKOVA, I. K. (1973). *Sov. Phys. Crystallogr.* **18**, 173–176.
SONCHIK, S. M., ANDREWS, L., & CARLSON, K. D. (1983). *J. Phys. Chem.* **87**, 2004–2011.
SRIVASTAVA, R. D., UY, O. M. & FARBER, M. (1972). *J. Chem. Soc. Faraday Trans.* 2, **68**, 1388–1392.
TAKÉUCHI, Y. & KUDOH, Y. (1977). *Z. Kristallogr.* **146**, 281–292.
TOLMACHEV, S. M. & RAMBIDI, N. G. (1973). *High Temp. Sci.* **5**, 385–394.
VEGA, A. J. & LUZ, Z. (1987). *J. Phys. Chem.* **91**, 365–373.
VON DREELE, R. B., JORGENSEN, J. D. & WINDSOR, C. G. (1982). *J. Appl. Cryst.* **15**, 581–589.
WAN, C., GHOSE, S. & GIBBS, G. V. (1977). *Am. Mineral.* **62**, 503–512.
WILLIAMS, P. P. & DENT GLASSER, L. S. (1971). *Acta Cryst.* B**27**, 2269–2275.
WOOLLEY, H. W. (1959). *Natl Bur. Stand. (US) Rep.* No. 6484, 40–44.
WOOLLEY, H. W., LIDE, D. R. & EVANS, W. H. (1959). *Natl Bur. Stand. (US) Rep.* No. 6484, 45–48.

Acta Cryst. (1988). B**44**, 334–340

New Analysis of the Neutron Diffraction Data for Anhydrous Orthophosphoric Acid and the Structure of H_3PO_4 Molecules in Crystals

BY ROBERT H. BLESSING

Medical Foundation of Buffalo, 73 High Street, Buffalo, New York 14203, *USA*

(*Received* 14 *September* 1987; *accepted* 2 *February* 1988)

Abstract

Two neutron data sets, which had been analyzed separately to determine the H-atom positions in H_3PO_4 crystals [Cole (1966). PhD Thesis, Univ. of Washington, Pullman, USA], have been re-analyzed in a joint refinement, fitting separate scale and extinction parameters for each data set, in order to obtain more precise positional and vibrational parameters. The new refinement gave $R(F) = 0{\cdot}036$ for the combined 743 data. For the new results, and for six other H_3PO_4 molecules from four other, different crystal structures, thermal vibration analyses have been performed, and the molecular structures, thermal vibrations and hydrogen-bonding effects are compared. The rigid-body model is found to be better than the riding model for the PO_4 groups. The P—OH bond lengths are markedly affected by hydrogen bonding, but seem to be independent of O=P—O—H conformation. These effects are interpreted in terms of the P—O partial double-bond character. Crystal data (Cole, 1966): anhydrous orthophosphoric acid, H_3PO_4, $M_r = 98{\cdot}00$, room temperature, $P2_1/c$, $a = 5{\cdot}779$ (9), $b = 4{\cdot}826$ (4), $c = 11{\cdot}606$ (40) Å, $\beta = 95{\cdot}26$ (18)°, $V = 322{\cdot}3$ (20) Å^3, $Z = 4$, $D_x = 2{\cdot}019$ mg mm^{-3}, $\mu = 0{\cdot}1687$ mm^{-1} for neutrons with $\lambda = 1{\cdot}450$ Å.

Introduction

The general features of the H_3PO_4 crystal structure were worked out from two-dimensional X-ray data by Smith, Brown & Lehr (1955) and, independently, by Furberg (1955). The H-atom positions were determined from three-dimensional neutron data by Cole (1966) [see also Cole & Peterson (1964)].

Cole (1966) carried out separate structure refinements against two neutron data sets measured at different wavelengths. One refinement, against 482 data with $(\sin\theta_{max})/\lambda = 0{\cdot}56$ Å^{-1} at $\lambda = 1{\cdot}450$ Å, gave R

0108-7681/88/040334-07$03.00

$= \sum||F_o|^2 - k^2|F_c|^2|/\sum|F_o|^2 = 0.058$ and $wR = [\sum w(|F_o|^2 - k^2|F_c|^2)^2/\sum w(|F_o|^2)^2]^{1/2} = 0.082$ with 55 of the largest $|F_o|^2$ omitted from the calculations because they were thought to suffer severe extinction. The other refinement, against 261 data with $(\sin\theta_{max})/\lambda = 0.46$ Å^{-1} at $\lambda = 1.078$ Å, gave $R = 0.045$ and $wR = 0.081$ with 30 of the largest $|F_o|^2$ omitted. For both refinements, $w = 1/\sigma^2(|F_o|^2)$ with $\sigma^2(|F_o|^2) = \sigma^2_{count} + (0.02|F_o|^2/\sin 2\theta)^2$, and the neutron-scattering length of phosphorus was treated as a variable parameter. Atomic positions from the two refinements agreed within experimental error, but there were significant differences between thermal vibration parameters.

We have carried out a new refinement against the combined 743 data of the two data sets, fitting separate scale and extinction parameters for each set, and using more recent and precise values for the neutron-scattering lengths (Koester, 1977). It turns out that the extinction is not very serious – only some 30 unique reflections had intensities smaller than 90% of their kinematic values – and a simple isotropic extinction model provides adequate corrections. Owing to the extinction corrections and the larger data-to-parameter ratio in the new refinement, the precision of the results, especially the thermal vibration parameters, is improved.

Experimental data

Neutron diffraction data were measured by S. W. Peterson at Oak Ridge National Laboratory as described by Cole (1966): BF_3 counter, Be monochromator crystal, NaCl crystal for wavelength and intensity calibrations, room temperature. H_3PO_4 specimen crystals of approximately rectangular parallelopiped shape, approximately 2 mm on an edge, sealed in thin-walled glass capillaries to protect the very hygroscopic crystals against atmospheric moisture. Lattice parameters by least-squares fit to $(\sin\theta)^2$ values for 45 reflections. Intensity data measured by $\theta/2\theta$ step scans in a fixed-count-per-step timing mode. Two data sets measured at different wavelengths: 482 unique reflections, $0 \le h \le 6$, $0 \le k \le 5$, $-12 \le l \le 12$, and $(\sin\theta)/\lambda \le 0.563$ Å^{-1} at $\lambda = 1.450$ Å; and 261 unique reflections, $0 \le h \le 5$, $0 \le k \le 4$, $-10 \le l \le 10$, and $(\sin\theta)/\lambda \le 0.464$ Å^{-1} at $\lambda = 1.078$ Å. Absorption corrections by Gaussian numerical quadrature.

Cole (1966) tabulated the $|F_o|^2$ values for the two data sets, but he did not list the corresponding experimental error estimates, $\sigma(|F_o|^2)$. For the new analysis, $\sigma(|F_o|^2)$ values were estimated from the root-mean-square deviations, $s = [\sum_{i=1}^{n}(x_i - \langle x\rangle)^2/(n-1)]^{1/2}$, for the $n = 2$ measurements of $x = |F_o|^2$ for the 261 reflections common to the two data sets. When the two sets were scaled together (Hamilton, Rollett & Sparks, 1965) and the duplicate data were averaged, the normalized root-mean-square deviation, $R_{int} = [\sum(x - \langle x\rangle)^2/\sum x^2]^{1/2}$, was 0.024 and the s *versus* x data for $x < 1000$ could be fitted quite well by a least-squares cubic polynomial, $s = 9.63 - 0.0417x + 1.84 \times 10^{-4}x^2 - 1.03 \times 10^{-7}x^3$. These calculated s values were taken to be fair estimates of $\sigma(|F_o|^2)$ for $|F_o|^2 < 1000$, and for the larger $|F_o|^2$, $\sigma(|F_o|^2) = [50^2 + (0.02|F_o|^2)^2]^{1/2}$ was assumed. There were 667 data with $|F_o|^2 > 2\sigma(|F_o|^2)$.

Least-squares refinement

The quantity minimized was $\chi^2 = \sum w(|F_o|^2 - k^2y|F_c|^2)^2$, where $w = 1/\sigma^2(|F_o|^2)$, k is a scale factor and $y = (1 + 2x)^{-1/2}$ with $x = g|F_c|^2/\sin 2\theta$ is a simplified Darwin–Zacharaisen extinction factor. The extinction parameter g, which was treated as an isotropic constant, is an approximation to a complicated function of the radiation wavelength, the absorption-weighted mean path length of the incident and scattered beams through the crystal for each reflection, and the mean radius and mean angular misorientation of the perfect crystal domains in the hypothetical mosaic crystal. The isotropic constant approximation gives reasonable extinction corrections in the case of small extinction in a weakly absorbing crystal of roughly spherical shape. The refinement converged with $wR = [\chi^2/\sum w(|F_o|^2)^2]^{1/2} = 0.0642$, $R = wR|_{w=1} = 0.0473$, and $S = [\chi^2/(m-n)]^{1/2} = 1.406$ for the $m = 743$ data and $n = 76$ parameters, which included the values $k = 1.103$ (5) and 1.029 (5) and $g = 5.9$ (4) and 5.8 (4) $\times 10^{-6}$ fm^{-2} for the $\lambda = 1.450$ and 1.078 Å extinction factor, $y = 0.692$. In the final least-squares cycle, the largest shift-to-e.s.d. ratio was < 0.001, and values of $\langle\chi_i^2/n_i\rangle^{1/2}$ for levels of h, k and l and for shells of $(\sin\theta)/\lambda$ and $|F_c|^2$ magnitude were roughly constant, averaging 1.3 and varying randomly from 1.0 to 2.1.

Results and discussion

The final positional and thermal vibration parameters are given in Tables 1 and 2.* The crystal structure is illustrated in Fig. 1, and the atom labeling, thermal vibrations and hydrogen-bonded surroundings of a molecule are shown in Fig. 2.

* Tables of $|F_o|^2$, $|F_c|^2$ and $\sigma(|F_o|^2)$ for the neutron data sets at the two wavelengths, and tables of thermal vibration corrected P–O and O–H bond lengths, H···O hydrogen-bond distances, O=P–O–H conformation angles, and P–O–H valence angles for H_3PO_4 molecules in crystals have been deposited with the British Library Document Supply Centre as Supplementary Publication No. SUP 44731 (12 pp.). Copies may be obtained through The Executive Secretary, International Union of Crystallography, 5 Abbey Square, Chester CH1 2HU, England.

Table 1. *Fractional atomic coordinates*

	x	*y*	*z*
H2	0·4762 (3)	0·6209 (3)	0·17724 (16)
H3	−0·1332 (3)	0·4715 (4)	0·17155 (16)
H4	0·2694 (4)	−0·0641 (5)	0·04118 (19)
O1	0·28353 (15)	0·16456 (20)	0·25338 (9)
O2	0·32299 (19)	0·58820 (19)	0·12924 (9)
O3	−0·05689 (15)	0·34116 (21)	0·11965 (9)
O4	0·27505 (17)	0·13175 (27)	0·03427 (8)
P	0·20925 (15)	0·30035 (20)	0·14029 (8)

Table 2. *Thermal vibration amplitudes* (Å²)

$$F(\mathbf{h}) = F_o(\mathbf{h}) \exp\left(-2\pi^2 \sum_{i=1}^{3} \sum_{j=1}^{3} h_i h_j a_i^* a_j^* U_{ij}\right).$$

	U_{11}	U_{22}	U_{33}	U_{12}	U_{13}	U_{23}
H2	0·0347 (10)	0·0299 (9)	0·0397 (10)	−0·0046 (7)	−0·0063 (9)	0·0001 (7)
H3	0·0267 (8)	0·0439 (10)	0·0420 (11)	0·0054 (8)	−0·0018 (7)	−0·0066 (9)
H4	0·0658 (13)	0·0320 (14)	0·0682 (15)	0·0009 (10)	0·0201 (10)	−0·0140 (10)
O1	0·0219 (5)	0·0292 (5)	0·0254 (6)	−0·0015 (4)	−0·0041 (4)	0·0069 (4)
O2	0·0288 (6)	0·0169 (5)	0·0335 (6)	−0·0030 (4)	−0·0111 (5)	0·0029 (4)
O3	0·0179 (5)	0·0321 (6)	0·0314 (6)	0·0038 (4)	−0·0054 (4)	−0·0087 (5)
O4	0·0374 (6)	0·0251 (7)	0·0274 (6)	0·0041 (5)	0·0075 (4)	−0·0053 (4)
P	0·0170 (5)	0·0169 (6)	0·0203 (6)	0·0015 (4)	−0·0029 (4)	0·0005 (4)

Crystal packing and hydrogen bonding

The hydrogen-bond geometries are given in Table 3. The H—O—P valence angles are 116·8 (3), 118·2 (3) and 116·2 (2)°, and the H—O—P—O1 conformation angles are 25·0 (2), 65·8 (2) and 34·8 (2)°, at O2, O3 and O4, respectively. The phosphoryl oxygen, O1, accepts two short, strong hydrogen bonds from the phosphohydroxyl groups, O2—H and O3—H. The third phosphohydroxyl group is the donor in one relatively weak hydrogen bond, O4—H···O2′, and in a second, very weak interaction, O4—H···O3′. Thus O2—H and O3—H are both donors and acceptors, but O4—H is a donor only, in an unusual, three-center hydrogen bond. Around O1, O2 and O3 the arrangement of the P atom and the covalently and hydrogen-bonded H atoms is approximately trigonal planar, as is the arrangement of O atoms around H4 (Fig. 2).

The three stronger hydrogen bonds link the molecules into corrugated layers stacked along **c** at $z = \frac{1}{4}$ and $\frac{3}{4}$ (Fig. 1). The only hydrogen bond between the layers is the long, weak O4—H···O3′ interaction; otherwise, the layers are in van der Waals contact. The closest of these contacts involves a side-by-side arrangement of antiparallel O4—H groups from adjacent layers. These groups are oriented about perpendicular to, and arrayed along, $[x,\frac{1}{2},\frac{1}{2}]$ in a zig-zag chain, which is shown end-on at the center of Fig. 1(*b*). Cooperative reinforcement of the bond polarizations along this chain of antiparallel $O^{\delta-}$—$H^{\delta+}$ bond dipoles is presumably a significant component of the interlayer bonding. The distances within the parallelogram-shaped links in the chain of dipoles are 2·868 (5) (O4···H4′ and H4···O4′), 2·977 (5) (H4···H4′) and 3·064 (4) Å (O4···O4′); the O4—H4···O4′ angle is 92·8 (2)°, and H4—O4···H4′ is 87·2 (2)°.

Molecular structure and thermal vibrations of H_3PO_4 *molecules in crystals*

The H_3PO_4 molecule occurs not only in crystals of anhydrous phosphoric acid (m.p. 315 K) but also in a crystalline phosphoric acid hemihydrate, $2H_3PO_4.H_2O$ (m.p. 302 K) (Smith, Brown & Lehr, 1955; Mighell, Smith & Brown, 1969; Dickens, Prince, Schroeder & Jordan, 1974). The molecule also occurs co-crystallized in a hydrogen-bonded adduct with acetic acid, $CH_3CO_2H.H_3PO_4$ (m.p. 307·5 K) (Jönsson, 1972), as a strongly hydrogen-bonded, almost ionized adduct with

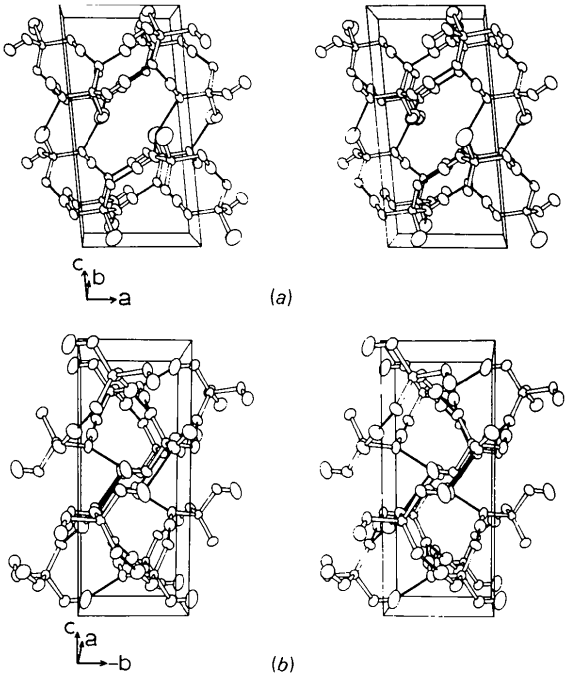

Fig. 1. Stereoscopic drawings (Johnson, 1971) of the H_3PO_4 unit cell.

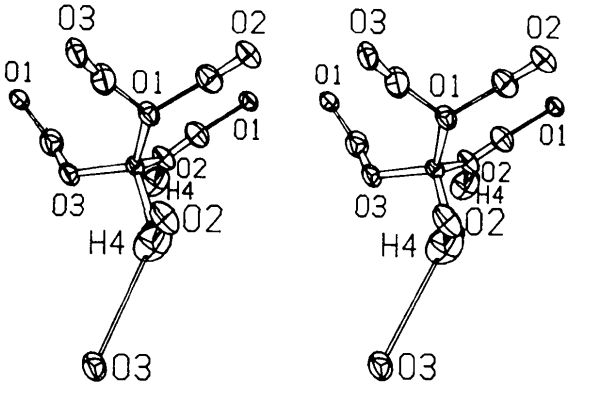

Fig. 2. Stereoscopic drawing (Johnson, 1971) of the H_3PO_4 molecule and its hydrogen-bonded surroundings in the crystal. The thermal vibration ellipsoids are 50% equiprobability surfaces. The orientation of the crystallographic axes is as in Fig. 1(*a*).

Table 3. *Hydrogen-bond distances* (Å) *and angles* (°)

O–H uncorrected/corrected* distance.

H···O / O···O uncorrected/lower limit†/independent-motion distance.

	O–H	H···O	O···O	O–H···O
O2–H2···O1′	1·014 (2)	1·554 (3)	2·568 (4)	177·5 (4)
	1·001	1·555	2·568	
		1·599	2·592	
O3–H3···O1″	1·001 (3)	1·588 (3)	2·584 (4)	173·0 (4)
	0·989	1·589	2·584	
		1·630	2·606	
O4–H4···O2′	0·950 (3)	1·974 (3)	2·849 (3)	152·2 (2)
	0·965	1·976	2·849	
		2·018	2·871	
O4–H4···O3′		2·522 (5)	3·095 (4)	118·9 (2)
		2·523	3·095	
		2·556	3·114	

* The O–H bond lengths are corrected for the sum of rigid-body libration effects, $\Delta d = d(L_{xx} + L_{yy})/2$ (Schomaker & Trueblood, 1968; Johnson, 1970; Johnson & Levy, 1974); riding-motion effects, $\Delta d = A\langle u_\pi^2\rangle/2d$ (Busing & Levy, 1964; Johnson, 1970; Johnson & Levy, 1974); and anharmonic bond-stretching effects, $\Delta d = -(3/2)a\Delta\langle u_\sigma^2\rangle$ (Ibers, 1959; Craven & Swaminathan, 1984; Jeffrey & Ruble, 1984). The quantity $(L_{xx} + L_{yy})/2$ represents the average of the mean-square angular displacements about the x and y axes of a Cartesian axial system with its z axis along the bond. The quantity $\langle u_\pi^2\rangle/2$ is the average mean-square atomic displacement perpendicular to the bond, and $\langle u_\sigma^2\rangle$ is the mean-square atomic displacement along the bond. A Morse-function asymmetry factor $a = 2$ Å^{-1} was assumed to hold as well for O–H bonds as it does for C–H bonds.

† The H···O and O···O distances are corrected to the lower limit values, which assume perfectly correlated parallel motion, $\Delta d = A^2(\langle u_\pi^2\rangle^{1/2})/2d$, and to the mean interatomic distance values assuming independent atomic vibrations, $\Delta d = \sum\langle u_\pi^2\rangle/2d$ (Busing & Levy, 1964; Johnson, 1970).

urea, $(NH_2)_2CO.H_3PO_4$ (Kostansek & Busing, 1972; Mootz & Albrand, 1972), and as a solvate molecule of crystallization in a dihydrogen phosphate salt of the amino acid L-histidine, $HisH^+.H_2PO_4^-.H_3PO_4$ (Blessing, 1986, 1987).

All of these crystal structures have been analyzed by neutron diffraction, except the histidine phosphate salt, which was the subject of a reasonably accurate X-ray study. Molecular geometries for the seven different H_3PO_4 molecules in the five different crystal structures are summarized in Tables 4 and 5. The atom numbering in the tables is not that used in the original structure determinations, rather it follows the sequence of the P–O bond lengths, as in the anhydrous H_3PO_4 structure (Fig. 2 and Table 4).

Thermal vibration analyses (Trueblood, 1984) were performed for the seven molecules using both the riding model of Busing & Levy (1964) and the rigid-body model of Schomaker & Trueblood (1968). Interatomic distances corrected for independent motion, riding motion and rigid-body libration are included in Tables 4 and 5, which show that the riding model and the rigid-body libration model give practically the same P–O bond-length corrections, and that the average P–O and O···O distances are constant within experimental error from molecule to molecule. The constancy of the average P–O distances indicates that while the phosphoryl bond lengths vary from 1·495 to 1·515 Å and the phosphohydroxyl bond lengths from 1·530 to 1·577 Å, the average or total P–O bond strength remains constant. The observed variations in P–O and O···O distances in the H_3PO_4 molecules are consistent with the results reported by Baur (1970,

Table 4. P–O *bond lengths* (Å) *in* H_3PO_4 *molecules in crystals*

Values given are uncorrected/riding-corrected/libration-corrected distances.

	P=O1 short	P–O2H longer	P–O3H longer	P–O4H longest	⟨P–O⟩
H_3PO_4	1·494 (4)	1·547 (2)	1·547 (3)	1·551 (4)	
	1·502	1·556	1·556	1·563	
	1·502	1·556	1·556	1·562	1·544
$2H_3PO_4.H_2O$	1·497	1·542	1·552	1·553	
	1·508	1·553	1·560	1·568	
	1·508	1·554	1·562	1·566	1·548
	1·486	1·545	1·556	1·556	
	1·494	1·557	1·564	1·568	
	1·495	1·556	1·565	1·566	1·546
$(CH_3CO_2H.H_3PO)_2$	1·486	1·538	1·545	1·549	
	1·496	1·551	1·558	1·564	
	1·498	1·550	1·559	1·564	1·543
	1·492	1·527	1·534	1·549	
	1·500	1·561	1·549	1·582	
	1·503	1·556	1·555	1·577	1·548
$(NH_2)_2CO.H_3PO_4$	1·506	1·520	1·552	1·560	
	1·510	1·530	1·564	1·570	
	1·515	1·530	1·565	1·573	1·546
$HisH^+.H_2PO_4^-.H_3PO_4$	1·489	1·544	1·545	1·556	
	1·496	1·556	1·562	1·576	
	1·502	1·553	1·560	1·574	1·547

Reported e.s.d.'s are 0·001 to 0·0015 Å in the hemihydrate structure (Dickens *et al.*, 1974), 0·003 Å in the acetic acid (Jönsson, 1972) and urea (Kostansek & Busing, 1972) complexes, and 0·002 Å in the histidine phosphate salt (Blessing, 1987). In the hemihydrate and acetic acid complex crystals, there are two H_3PO_4 molecules per crystal-chemical unit. The average and sample e.s.d. for the ⟨P–O⟩ values is 1·5460 ± 0·0019 Å.

Table 5. O–P–O *bond angles* (°) *and* O···O *distances* (Å) *in* H_3PO_4 *molecules in crystals*

Values given are the bond angle and uncorrected/libration-corrected/independent-motion distances.

	O1=P–O2H	O1=P–O3H	O1=P–O4H	HO2–P–O3H	HO2–P–O4H	HO3–P–O4H	⟨O–O⟩
H_3PO_4	112·1 (3)	113·2 (3)	113·3 (3)	107·3 (3)	105·6 (2)	104·9 (2)	
	2·523 (3)	2·539 (4)	2·554 (8)	2·492 (3)	2·467 (3)	2·456 (3)	
	2·538	2·552	2·560	2·506	2·483	2·473	2·519
	2·546	2·563	2·556	2·515	2·493	2·481	2·527
$2H_3PO_4.H_2O$	111·8	112·2	114·4	108·0	106·2	103·8	
	2·517	2·531	2·561	2·503	2·475	2·444	
	2·537	2·549	2·579	2·519	2·497	2·464	2·524
	2·546	2·555	2·586	2·528	2·504	2·470	2·532
	107·3	114·7	110·5	108·6	110·6	105·1	
	2·441	2·560	2·499	2·518	2·553	2·470	
	2·459	2·576	2·513	2·535	2·568	2·488	2·523
	2·467	2·582	2·524	2·541	2·575	2·494	2·531
$(CH_3CO_2H.H_3PO_4)_2$	109·3	114·1	112·7	110·4	105·6	104·4	
	2·466	2·544	2·526	2·531	2·459	2·445	
	2·485	2·566	2·549	2·552	2·481	2·466	2·516
	2·508	2·579	2·559	2·565	2·497	2·482	2·532
	108·5	115·5	111·9	110·0	108·6	102·0	
	2·450	2·560	2·520	2·509	2·498	2·396	
	2·483	2·579	2·551	2·554	2·545	2·441	2·526
	2·503	2·594	2·567	2·558	2·547	2·446	2·536
$(NH_2)_2CO.H_3PO_4$	113·7	106·9	112·0	110·8	105·1	108·3	
	2·534	2·458	2·542	2·528	2·446	2·523	
	2·548	2·474	2·559	2·547	2·466	2·543	2·523
	2·560	2·488	2·566	2·557	2·475	2·552	2·533
$HisH^+.H_2PO_4^-.H_3PO_4$	114·5	113·9	112·4	102·1	105·3	107·8	
	2·551	2·543	2·530	2·402	2·465	2·506	
	2·568	2·567	2·557	2·419	2·486	2·533	2·525
	2·578	2·572	2·558	2·437	2·500	2·536	2·530

Literature citations and e.s.d.'s of the interatomic distances are given in Table 4. Corrections for the O···O distances to the lower limit values were always <0·001 Å. The average and sample e.s.d. for the ⟨O–O⟩ values is 2·5223 ± 0·0035 Å for the libration-corrected distances, and 2·5316 ± 0·0028 Å for the independent-motion distances.

1974) in his comprehensive studies of the distortions of 211 phosphate groups in 129 crystal structures. Baur showed that most of the variation in geometry correlates with variation in bond strengths calculated from electrostatic valence rules.

The main deviation of the PO_4 groups in the H_3PO_4 molecules from regular tetrahedral geometry is an off-center displacement of the P atom along the ideal threefold axis to give one shorter P=O and three longer P—OH bonds. There also tends to be a secondary, smaller displacement of the P atom toward, or away from, one of the OH groups to give one shorter and two longer, or one longer and two shorter, P—OH bonds (Table 4). The P=O double bond and P—OH single bond designations are merely formal, and both types of bond possess variable partial double-bond character. Corresponding to the displacement of the central P atom, the three O=P—OH edges of the PO_4 tetrahedron tend to be longer and the three HO—P—OH edges shorter than the average O···O edge by ~0·03 Å (Table 5). This could indicate a slight expansion of the van der Waals radius of a non-protonated P=O oxygen, or contraction of the radius of a protonated P—OH oxygen, in directions transverse to the P—O bond. Such variations of the shape of the O atoms would be consistent with the theoretical H_3PO_4 deformation density shown in Fig. 3 (Moss & Blessing, 1984).

Riding motion versus rigid-body libration for the PO_4 *groups*

Since the atomic mass of phosphorus is almost twice that of oxygen, and since riding-motion bond-length corrections are easy to calculate, the riding model has been applied to phosphate groups quite often. Rigid-body thermal vibration analyses of phosphate groups have been carried out much less often. The dynamics of the two models are quite different: the riding model assumes more-or-less independent bond-bending vibrations of the phosphate oxygens superimposed on correlated translational vibrations of the phosphorus and oxygen together; the rigid-body model, as its name implies, assumes that all the atomic vibrations are perfectly correlated. Still, it is reasonable that the riding model and the rigid-body libration model give about equal corrections for the P—O bond lengths in PO_4 groups (Table 4), because the center of mass and the center of libration in a tetrahedral PO_4 group coincide at the P-atom position. Therefore, rigid-body PO_4 group librations are equivalent to correlated O-riding-on-P motions.

To assess the rigidity of the H_3PO_4 molecules in crystals, the rigid-bond test of Hirshfeld (1976) and the rigid-molecule test of Rosenfeld, Trueblood & Dunitz (1978) were performed. Summary results are given in Table 6. In most cases, the average values of $\Delta\langle u^2\rangle$ along the P—O and O···O directions are about equal to the corresponding $\sigma(\Delta)$ values; in the worst case, $\Delta/\sigma = 6$. Statistics of fit from the rigid-body analyses are summarized in Table 7. These show that, with the possible exception of the data from the acetic acid complex, the rigid-body models fit to within experimental error.

The statistical evidence that the PO_4 groups are rigid must be somewhat qualified, because the atomic

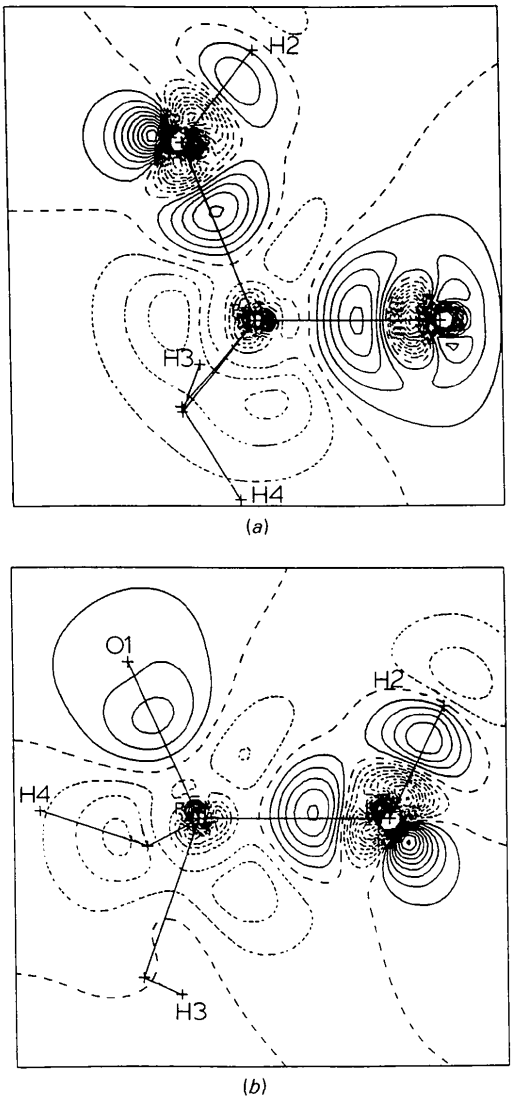

Fig. 3. Theoretical H_3PO_4 static deformation density maps, $\Delta\rho(\mathbf{r}) = \rho_m(\mathbf{r}) - \sum_a \rho_a^0(\mathbf{r} - \mathbf{r}_a)$, where ρ_m is the molecular electron density and $\sum_a \rho_a^0(\mathbf{r} - \mathbf{r}_a)$ is the superposition of spherically averaged free-atom electron densities: (*a*) an O=P—O(H) section; (*b*) a P—O—H section. Contour interval 0·1 e Å^{-3}; positive contours, solid; zero, dashed; and negative, dotted. Both ρ_m and the ρ_a^0 were calculated from SCF wavefunctions of split-valence-plus-polarization quality, which were equivalent to 6-31G**. The experimental molecular geometry from the anhydrous H_3PO_4 crystal structure was used for the SCF calculation; idealized $C_{3v} - 3m$ molecular symmetry was not imposed (Moss & Blessing, 1984).

Table 6. *Rigid-bond and rigid-molecule test results*

Average and maximum $\Delta\langle u^2\rangle = |\langle u_A^2\rangle - \langle u_B^2\rangle|$ and $\sigma(\Delta)$ (Å^2) along A–B interatomic directions.
Literature citations are given in Table 4.
Along the O–H bonds and the intramolecular H···O and H···P directions the values of $\Delta\langle u^2\rangle$ are five to ten times larger than the P–O and O···O values because, as Figs. 1 and 2 indicate, the amplitudes of the internal modes of O–H bond stretching and bending vibrations are comparable to the amplitudes of the external lattice-vibration modes.
The last column of the table lists the diffraction data-set resolution.

	P–O		O···O		$(\sin\theta_{max})/\lambda$
	avg.	max.	avg.	max.	(Å^{-1})
H_3PO_4	0·0009 (8)	0·0013 (8)	0·0013 (8)	0·0021 (8)	0·56
$2H_3PO_4.H_2O$	0·0010 (7)	0·0018 (8)	0·0018 (8)	0·0024 (8)	0·62
	0·0005 (7)	0·0012 (7)	0·0011 (7)	0·0027 (8)	
$(CH_3CO_2H.H_3PO_4)_2$	0·0025 (6)	0·0035 (7)	0·0019 (6)	0·0047 (8)	0·50
	0·0014 (6)	0·0045 (7)	0·0032 (8)	0·0052 (9)	
$(NH_2)_2CO.H_3PO_4$	0·0020 (15)	0·0026 (16)	0·0010 (15)	0·0025 (16)	0·73
$HisH^+.H_2PO_4^-.$ H_3PO_4	0·0018 (7)	0·0027 (10)	0·0010 (10)	0·0020 (13)	0·70

Table 7. *Selected results from the fit of rigid-body molecular* **TLS** *tensors to the independent-atom* **U** *tensors of the* PO_4 *groups of* H_3PO_4 *molecules*

$wR = \{\sum w[U_{ij} - U_{ij}(\mathbf{TLS})]^2/\sum w(U_{ij})^2\}^{1/2}$, where $w = 1/\sigma^2(U_{ij})$.
$\Delta_{r.m.s.} = \langle[U_{ij} - U_{ij}(\mathbf{TLS})]^2\rangle^{1/2}$.
$\sigma_{r.m.s} = \langle\sigma^2(U_{ij})\rangle^{1/2}$.
L_1, L_2 and L_3 designate the principal-axis librations.
The H atoms were omitted from the rigid-body fit on account of their large amplitudes of internal vibration.

		$\Delta_{r.m.s.}$	$\sigma_{r.m.s.}$	$\langle\omega^2\rangle^{1/2}$ (°)		
	wR	(Å^2)	(Å^2)	L_1	L_2	L_3
H_3PO_4	0·0307	0·00050	0·00050	5·2	4·6	3·4
$2H_3PO_4.H_2O$	0·0285	0·00057	0·00047	5·8	5·3	3·7
	0·0274	0·00048	0·00044	5·7	4·0	4·0
$(CH_3CO_2H.H_3PO_4)_2$	0·0288	0·00101	0·00035	5·9	5·3	4·7
	0·0252	0·00109	0·00042	10·3	4·9	4·3
$(NH_2)_2CO.H_3PO_4$	0·0477	0·00091	0·00092	5·9	4·6	3·6
$HisH^+.H_2PO_4^-.H_3PO_4$	0·0280	0·00091	0·00058	7·0	5·0	3·7

thermal vibration parameters are only moderately precise [$\sigma(U_{ij}) \cong 0{\cdot}0005$ Å^2], the main limitation being the restricted $(\sin\theta)/\lambda$ resolution of the diffraction data sets (Table 7). Thus the results given in Tables 6 and 7 do not rule out the possibility that small but significant amplitudes due to internal, molecular modes of bond-bending O-atom riding vibrations are superimposed on the amplitudes of the external, lattice modes of rigid-body PO_4 librations. Even so, the rigid-body model is certainly a better first approximation for the PO_4 groups than the riding model, which happens to give reasonable corrections for the P–O bond lengths simply because of the tetrahedral geometry of PO_4 groups. For the intramolecular O···O distances, Table 5 shows that the assumption of independent O-atom riding vibrations gives values that are too large by ~0·01 Å compared to the libration-corrected values.

Hydrogen-bonding effects on the P–O *bond lengths*

Although the average P–O bond length is constant in H_3PO_4 molecules in crystals, there is a variation of ~0·020 Å in P=O and ~0·045 Å in the P–OH distances in Table 4, due to crystal environmental effects. Fig. 4 shows that part of the variation is attributable to variation in the strengths of the hydrogen bonds formed by the H_3PO_4 molecules, which range from a short, strong, centered P–O–H···O=C interaction (O···O = 2·42 Å) in the urea–phosphoric acid complex to the long, weak interlayer P–O–H··· O(H)–P interaction (O···O = 3·10 Å) in the anhydrous phosphoric acid crystals.

The P–OH *versus* H···O data in Fig. 4 are consistent with a scheme of canonical structures,

$$\{\mathrm{P{-}O{-}H\cdots O{=}P} \longleftrightarrow \overset{(-)}{\mathrm{P}}{=}\overset{(+)}{\mathrm{O}}{-}\mathrm{H}\cdots\overset{(-)}{\mathrm{O}}{-}\overset{(+)}{\mathrm{P}}\},$$

which would predict that the P–OH bond should get shorter as the H···O acceptor bond gets shorter and weakens the O–H donor bond. This scheme, in fact, accounts for the general trend in the P–OH *versus* O–H···O data from some 100 hydrogen-bonded phosphate crystal structures (Ichikawa, 1987; Ferraris & Ivaldi, 1984), which fall along regression lines with about the same slope as in Fig. 4. The same scheme would predict that the P=O acceptor bond should get longer as the accepted O···H bond gets shorter, but, for the five P=O groups in H_3PO_4 molecules that are double acceptors of O···H–O hydrogen bonds, there is too little variation in the averages of the two O···H distances (1·572 ± 0·017 to 1·588 ± 0·032 Å) to establish any significant correlation with the variation in P=O bond lengths. Ichikawa (1987) has shown that as the P–OH bond lengths in $H_2PO_4^-$ and HPO_4^{2-} anions are shortened by stronger hydrogen-bond donation, the P=O bond lengths to the non-protonated oxygens are lengthened to maintain a constant average P–O bond strength. The constancy of the average bond lengths in Table 4 indicates that the H_3PO_4 molecules follow the same pattern.

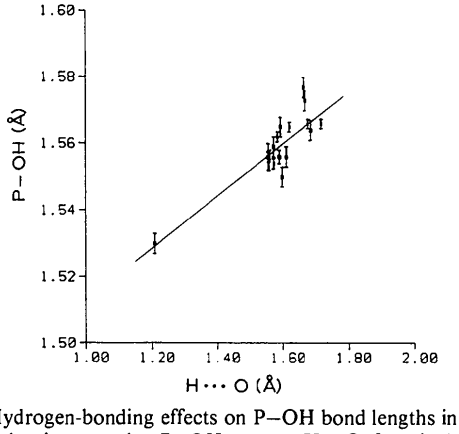

Fig. 4. Hydrogen-bonding effects on P–OH bond lengths in H_3PO_4 molecules in crystals: P–OH *versus* H···O for single donor P–OH groups, $n = 17$, $r = 0{\cdot}87$, $p(n,r) < 0{\cdot}001$. The quantity $p(n,r)$ is the probability of no correlation, *i.e.*, the probability that n random-number pairs would give a linear correlation coefficient as large as r. The data used to construct the plots have been deposited.

Conformational variation in H_3PO_4 molecules in crystals

The partial double-bond character in P–O bonds is attributable to overlap of filled $2p\pi$ orbitals of oxygen with empty but energetically accessible $3d\pi$ orbitals of phosphorus (Cruickshank, 1961). The orbital interaction diagrams sketched in Fig. 5 indicate that, for an oxygen $p\pi$ orbital oriented perpendicular to the plane of a P–O–H group, the $p\pi(OH) \rightarrow d\pi(P)$ overlap should be best at O–P–O–H conformation angles of 0, ± 90, or 180°. The crystallographic data on the P–OH bond lengths *versus* the O=P–O–H conformation angles in H_3PO_4 molecules are plotted in Fig. 6, but they do not show any systematic variation. Evidently, the decrease in $p\pi(OH) \rightarrow d(z^2)\pi(P)$ overlap as the O=P–O–H angle changes from 90 to 45°, for example, is compensated by the increase in $p\pi(OH) \rightarrow d(x^2 - y^2)\pi(P)$ overlap, and the orientation of the OH group can adjust more-or-less freely to the available hydrogen-bonding opportunities without weakening the P–OH bond. Likewise, because the $d(z^2)$ and $d(x^2 - y^2)$ phosphorus orbitals offer the possibility of overlap with $p\pi$ oxygen orbitals in either of two orthogonal orientations, the bond density in the phosphoryl bond and the lone-pair density around the phosphoryl oxygen both display cylindrical symmetry in sections (not shown here) perpendicular to the P–O1 bond in Fig. 3(*a*).

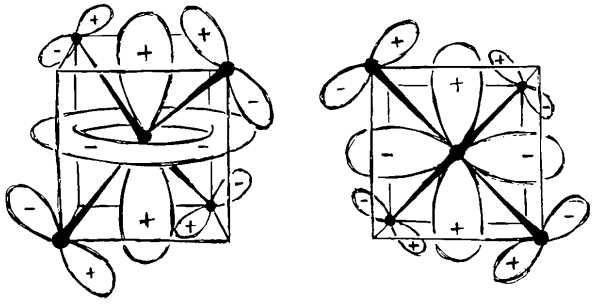

Fig. 5. Schematic diagrams of $p\pi(B) \rightarrow d\pi(A)$ orbital interactions in tetrahedral AB_4 molecules: left-hand diagram, $p\pi \rightarrow d(z^2)\pi$; right-hand diagram, $p\pi \rightarrow d(x^2 - y^2)\pi$. Adapted from Cruickshank (1961).

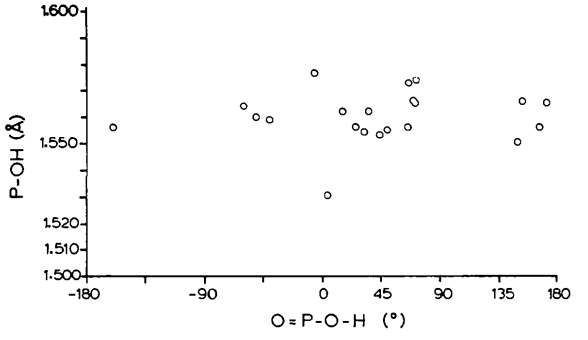

Fig. 6. Conformational variation in H_3PO_4 molecules in crystals. P–OH bond length *versus* O=P–O–H conformation angle. The data used to construct the plot have been deposited.

Mr Brian Tucker, a student assistant from Canisius College, helped will some of the data processing. Support from USDHHS PHS NIH grants Nos. GM34073 and DK19856 is gratefully acknowledged.

References

BAUR, W. H. (1970). *Trans. Am. Crystallogr. Assoc.* **6**, 129–155.
BAUR, W. H. (1974). *Acta Cryst.* B**30**, 1195–1215.
BLESSING, R. H. (1986). *Acta Cryst.* B**42**, 613–621.
BLESSING, R. H. (1987). *Acta Cryst.* B**43**, 407.
BUSING, W. R. & LEVY, H. A. (1964). *Acta Cryst.* **17**, 142–146.
COLE, F. E. (1966). PhD Thesis, Univ. of Washington, Pullman, USA. Ann Arbor, Michigan: Univ. Microfilms International.
COLE, F. E. & PETERSON, S. W. (1964). Am. Crystallogr. Assoc. Meet., Montana State Univ., Bozeman, Montana, July 1964, Abstract No. H-5.
CRAVEN, B. M. & SWAMINATHAN, S. (1984). *Trans. Am. Crystallogr. Assoc.* **20**, 133–135.
CRUICKSHANK, D. W. J. (1961). *J. Chem. Soc.* pp. 5485–5504.
DICKENS, B., PRINCE, E., SCHROEDER, L. W. & JORDAN, T. H. (1974). *Acta Cryst.* B**30**, 1470–1473.
FERRARIS, G. & IVALDI, G. (1984). *Acta Cryst.* B**40**, 1–6.
FURBERG, S. (1955). *Acta Chem. Scand.* **9**, 1557–1566.
HAMILTON, W. C., ROLLETT, J. S. & SPARKS, R. A. (1965). *Acta Cryst.* **18**, 129–130.
HIRSHFELD, F. L. (1976). *Acta Cryst.* A**32**, 239–244.
IBERS, J. A. (1959). *Acta Cryst.* **12**, 251.
ICHIKAWA, M. (1987). *Acta Cryst.* B**43**, 23–28.
JEFFREY, G. A. & RUBLE, J. R. (1984). *Trans. Am. Crystallogr. Assoc.* **20**, 129–132.
JOHNSON, C. K. (1970). In *Crystallographic Computing*, edited by F. R. AHMED, pp. 207 *ff.* Copenhagen: Munksgaard.
JOHNSON, C. K. (1971). *ORTEP*II. Report ORNL-3794, revised. Oak Ridge National Laboratory, Oak Ridge, Tennessee, USA.
JOHNSON, C. K. & LEVY, H. A. (1974). In *International Tables for X-ray Crystallography*, Vol. IV, edited by J. A. IBERS & W. C. HAMILTON, pp. 311 *ff.* Birmingham: Kynoch Press. (Present distributor Kluwer Academic Publishers, Dordrecht.)
JÖNSSON, P.-G. (1972). *Acta Chem. Scand.* **26**, 1599–1619.
KOESTER, L. (1977). In *Neutron Physics*, edited by G. HÖHLER. Berlin: Springer Verlag.
KOSTANSEK, E. C. & BUSING, W. R. (1972). *Acta Cryst.* B**28**, 2454–2459.
MIGHELL, A. D., SMITH, J. P. & BROWN, W. E. (1969). *Acta Cryst.* B**25**, 776–781.
MOOTZ, D. & ALBRAND, K.-R. (1972). *Acta Cryst.* B**28**, 2459–2463.
MOSS, G. R. & BLESSING, R. H. (1984). *Acta Cryst.* A**40**, C-157.
ROSENFELD, R. E., TRUEBLOOD, K. N. & DUNITZ, J. D. (1978). *Acta Cryst.* A**34**, 828–829.
SCHOMAKER, V. & TRUEBLOOD, K. N. (1968). *Acta Cryst.* B**24**, 63–76.
SMITH, J. P., BROWN, W. E. & LEHR, J. R. (1955). *J. Am. Chem. Soc.* **77**, 2728–2730.
TRUEBLOOD, K. N. (1984). *Trans. Am. Crystallogr. Assoc.* **20**, 15–22.